Minimizing Strong Telluric Absorption in Near-Infrared Stellar Spectra

MATTHEW A. KENWORTHY[1] AND MARGARET M. HANSON

Department of Physics, University of Cincinnati, Cincinnati, OH 45220; matt@physics.uc.edu

ABSTRACT. We have obtained high-resolution spectra ($R \sim 25{,}000$) of an A star over varying air mass to determine the effectiveness of telluric removal within the limit of a high signal-to-noise ratio. The near-infrared line He I at 2.058 μm, which is a sensitive indicator of physical conditions in massive stars, supergiants, H II regions, and YSOs, resides among pressure-broadened telluric absorption from CO_2 and water vapor that varies with both time and observed air mass. Our study shows that in the limit of bright stars at high resolution, accuracies of 5% are typical for high–air-mass observations (greater than 1.9), improving to a photon-limited accuracy of 2% at smaller air masses (less than 1.15). We find that by using the continuum between telluric absorption lines of a rovibrational fan, a photon-limited 1% accuracy is achievable.

1. INTRODUCTION

Our goal is to obtain high-quality, moderate-resolution spectra ($R \sim 10{,}000$–20,000) to be used in conjunction with sophisticated stellar model atmospheres (Santolaya-Rey, Puls, & Herrero 1997). The near-infrared (NIR) spectrum of the atmosphere from 1 to 5 μm is dominated by telluric water and CO_2 absorption, between which the major observing windows in the wavelength region are defined. Broad molecular absorption bands of CO_2 are resolved at moderate spectral resolution ($R > 5000$) into individual pressure-broadened rovibrational transitions. These transitions vary in both time and observed elevation, making their removal problematic in ground-based spectroscopic studies.

There is a tremendous impetus from astronomers to obtain highly accurate spectral profiles for lines existing in the near-infrared. For hot stars, an important line in the modeling of extended atmospheres and stellar winds is the He I transition at 2.058 μm (Hanson et al. 1996). This line is also an important diagnostic in H II regions (Lumsden et al. 2003), massive young stellar objects (Porter et al. 1998), and planetary nebulae (Depoy & Shields 1994; Lumsden et al. 2001). However, the line is located near the short-wavelength edge of the *K*-band window, where CO_2 absorption bands dominate the spectrum. The challenge for observational astronomers is to obtain observations of the 2.058 μm line profile with a high enough signal-to-noise ratio (S/N) to be suitable for detailed modeling despite considerable telluric contamination.

Observations of standard stars are essential to obtain even modest corrections of telluric absorption features in this spectral region. This paper investigates the variability of telluric absorption near the He I transition and discusses the limits to the S/N achievable given a typical observing program and instrument. We follow an A2 V star for half a night through a range of air masses and see what effect the variation of telluric absorption has on the recovered spectra.

2. OBSERVATIONS

The data were taken at the Infrared Telescope Facility (IRTF) on 2003 June 8, 0600 UT (2003 June 7, 2000 HST). Meteorological data from weather stations across the Mauna Kea summit are shown in Figure 1 along with the range of air masses observed. The observations started at an air mass of 1.95 and finished at an air mass of 1.13, when the star was approaching transit.

We used the Cryogenic Echelle Spectrograph (Greene et al. 1993) with a slit width of 1″.0. Combined with the pixel scale of 0″.2 pixel^{-1}, this gives a slit width of 5 pixels on the 256×256 (30 μm pitch) InSb array. The array has a read noise of 55 e^- pixel^{-1} per sample and a dark current of 0.5 e^- s^{-1} pixel^{-1}, with an approximate gain of 11 e^-/ADU. With a 325 mV bias, it is 1% linear at 22,000 e^-. One echelle order is selected with an order-sorting filter, and the dispersion is 0.20 Å pixel^{-1}. Due to problems with the telescope guiding camera, the telescope is off-axis guided by a nearby star, in contrast to the usual mode of on-axis guiding with the target star in visible light.

The dispersion of the spectrograph at 2.0563 μm is measured at 0.207 Å pixel^{-1}. The instrumental spectral resolving power is measured by fitting a Gaussian to two OH night sky emission lines, identified as a Λ *P*1 doublet (Rousselot et al. 2000), with a full width at half-maximum of 4.0 pixels (12.1 km s^{-1}) and with the star overfilling the slit. This gives a higher spectral resolution than expected with the stated slit width, so we take

[1] Steward Observatory, 933 North Cherry Avenue, Tucson, AZ 85721.
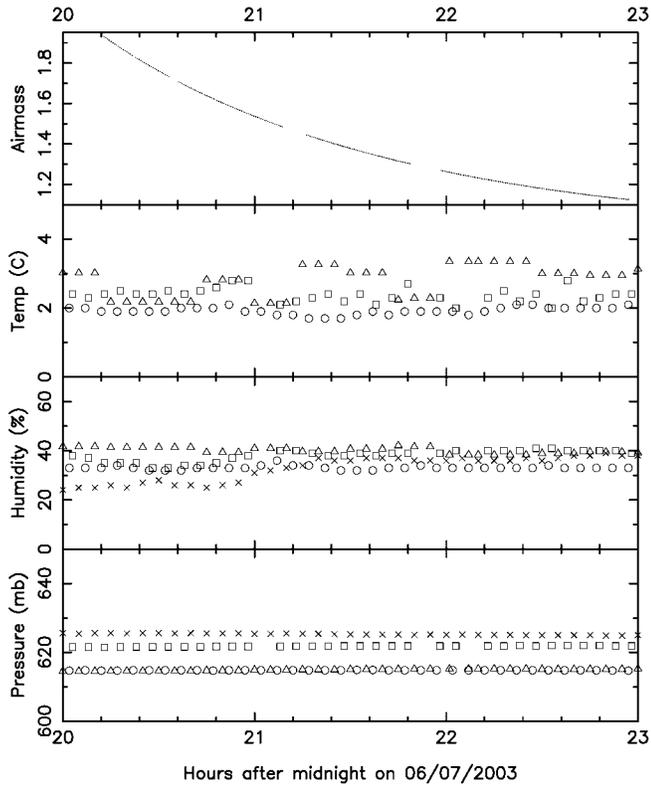
FIG. 1.—Meteorological conditions from different telescope weather stations across the summit of Mauna Kea. Canada−France−Hawaii Telescope (CFHT) data are marked with a circle, Caltech Submillimeter Observatory (CSO) data with a cross, Subaru with a square, and United Kingdom Infrared Telescope (UKIRT) data with a triangle. Data provided by Mauna Kea Weather Center (Lyman 2003, private communication).

our measured value of the dispersion and instrumental width to obtain a spectral resolution of 24,800.

A dwarf A2 star is not expected to have any significant metal lines in its spectrum, and as a result acts as a continuum source above the atmosphere over the spectral region of the study. The A2 V star HD 156729 ($17^h17^m40\!\!^s2545$, $+37°17'29\!\!''39$, J2000.0, $V = 4.62$) is followed from an air mass of 1.95 through to 1.13, with 30 s integrations in a continuous beam-switching mode with a throw of $9\!\!''0$. The mean time between the start of successive observations is 34 s, resulting in 268 fully reduced observations.

We set the central wavelength of the spectra to 2.061 μm to include a range of different line strengths. Three P-branch transitions, the Q transition, and four R-branch transitions of CO_2 are included in the spectra, along with some H_2O transitions (see Fig. 2).

A set of 20 flat fields is taken immediately after the end of the observations, using a continuum lamp placed in front of the entrance slit of the spectrograph. Dark frames of identical duration to the flat-field exposures are taken later in the night.
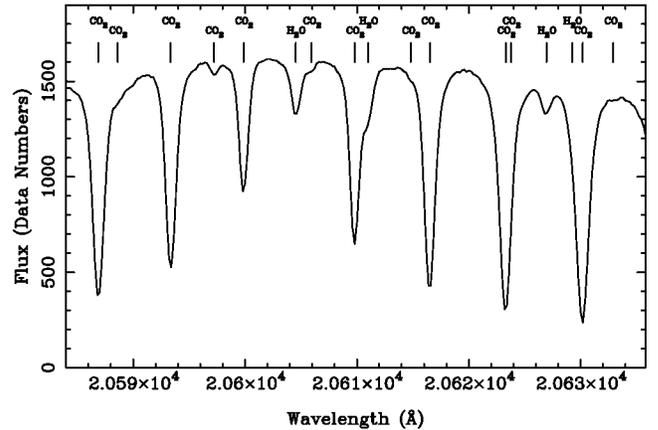
FIG. 2.—Spectrum of an A2 V star averaged from 10 exposures at a mean air mass of 1.13. All spectral features are due to telluric absorption in the Earth's atmosphere. Lines are identified according to the HITRAN database (Rothman et al. 2003). The Echelle transmission function has not been removed from the spectrum.

3. REDUCTION OF THE ECHELLE SPECTRA

All spectra are reduced using IRAF[2] routines, and subsequent analysis is done using Perl Data Language.[3]

The dark frames and flat-field frames are averaged together to form a master dark frame and master flat frame, and frames showing the rms per combined pixel (σ frames) are produced. The master dark frame is subtracted from the master flat-field frame, and the flat field is normalized in the spectral direction to produce a pixel response frame. Bright, noisy, and dead pixels are identified using the σ frames, and a bad-pixel frame is generated for the detector. Pairs of science frames are subtracted from each other, divided by the pixel response frame, and then bad pixels flagged in the bad-pixel frame are interpolated over using data from the surrounding good pixels.

There are two spectra per beam-switched frame. A fixed aperture width of 24 pixels (corresponding to $4\!\!''8$) is used to extract the spectra from the frame. Although in ideal beam switching the frame background level is zero, we noted in four pairs of beam-switched frames that a jump in bias level in the readout of the frame would result in a zero-level offset of up to 20 counts being present in the data, compared with the typical flux of 200 counts pixel^{-1} in the spectrum. Visual examination of these images shows a very smooth background that is automatically subtracted as part of the spectral extraction. Remaining transient events are removed with the CLEAN algorithm in the spectral extraction package, using the known gain

and effective read noise of the beam-switched images. The centroid position of the spectra are traced with a third-order Legendre function.

Wavelength dispersion correction is performed using the telluric profiles themselves. A model of the atmospheric transmission is generated for the observing site using ATRAN (Lord 1992), and all absorption-line profiles are measured from this reference. These are then used to wavelength-calibrate the individual spectra. Using a second-order Legendre function, a wavelength solution with an rms fit of 0.03 Å is typical, corresponding to a goodness of fit of about 1/10 of a pixel. The absorption lines are labeled according to the HITRAN database (Rothman et al. 2003) in Figure 2.

4. OBSERVING TECHNIQUE

The telluric absorption in the NIR varies as a function of air mass and of time (Tokunaga 1999). Ideally, in spectral regions of strong telluric absorption, a standard star and a science target should be observed through identical atmospheric paths at the same time, allowing the atmospheric absorption to be divided out. In this ideal case, a reference star would be within a few arcseconds of a science target, and placing the spectrograph slit across both objects in a position suitable for beam switching would result in the highest observing efficiency and accuracy.

Bright stars with no metallic lines (usually those later than B8 V and earlier than A2 V) are the most appropriate for telluric removal. They are not perfect, in that these stars have broad hydrogen lines in their spectra, so to obtain science target spectra in these regions, various modeling techniques have been developed (Maiolino et al. 1996; Hanson et al. 1996; Vacca et al. 2003) to remove the hydrogen lines from the standard star spectra while preserving the (much narrower) telluric absorption lines.

4.1. Standard Star Observations at Different Air Masses

A complete observation consists of obtaining spectra of the science target, slewing the telescope to a nearby standard star, and taking spectra of the standard star. The standard star and science target observations are separated both in time and position on the sky, and so are observed through different paths in the atmosphere. Differences in telluric absorption between these two pointings result in systematic errors appearing in the science object spectra, and these can significantly reduce the S/N and sensitivity reached in the object spectrum. This is shown in Figure 3, where the ratios of two standard star spectra at 1.13 and 1.94 air mass, respectively, are shown. The two lower spectra show the ratio of spectra taken approximately 35 s apart, with the lowest spectrum at 1.13 air mass and the middle spectrum at 1.94 air mass. The spectra show a flat, Gaussian noise–dominated continuum with spikelike residuals located at the cores of telluric absorption lines. This effect is seen in
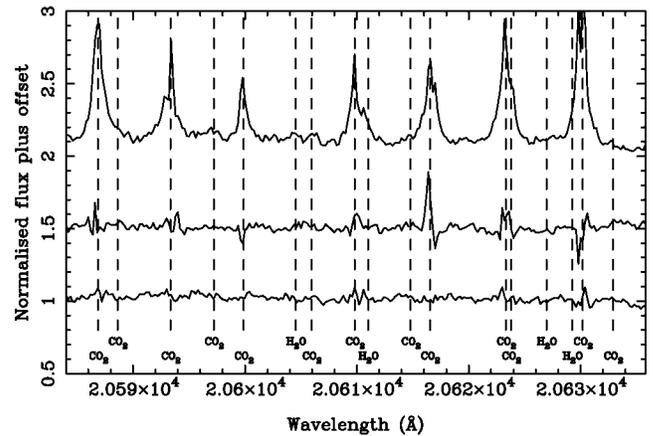
FIG. 3.—Ratio of two spectra of the same star taken at different air masses. The lowest spectrum is the division of two spectra taken at an air mass of 1.13; the middle spectrum is the division of spectra taken at an air mass of 1.94; and the top spectrum shows the division of a spectrum at an air mass of 1.13 by a spectrum at 1.94. Each spectrum has been offset by a flux of 0.5, and the dashed lines mark the center of telluric absorption lines and their associated molecular species.

greater detail in the topmost spectrum, where the ratio is between a spectrum from 1.13 and 1.94 air mass.

The rms value of such normalized spectra is a measure of the standard deviation of the spectrum from its mean value. Various sources of noise combine in quadrature to give the theoretical lowest noise limit attainable for a given spectral element in the final spectrum. For our ratio target spectra, we calculate a theoretical S/N and compare it to the measured S/N. The noise sources we include in the calculation of the theoretical noise limit are detector read noise, photon-count noise, and flat-field noise. For our extraction width of 24 pixels, this corresponds to a read noise of 380 e^- per wavelength bin of a beam-switched image, and our flat-field S/N is approximately 1200.

The increase in air-mass difference between the two spectra leads to lower S/N, as seen in Figure 4. At low air mass, the theoretical limit of 2.3% is reached for exposures taken 1 minute apart (*filled circles*). However, at a higher air mass of 1.94 (*open circles*), its theoretical limit of 2.6% is *not* reached, and instead the noise tails off at 5%, a S/N of only 20. Considering the significant telluric residuals for 1.94 air mass in the middle spectrum of Figure 3, it is apparent that the lowest possible air mass should be used for both standard and science objects.

We also examine the standard deviation of the spectrum as a function of air mass difference for a region of the spectrum with small telluric absorption, 2.0602–2.0608 μm. The theoretical noise limit of 1% is reached (Fig. 5), and for large air mass differences there is only a small decrease in S/N. Clearly, high S/N infrared spectra are obtainable in regions free of telluric absorption.
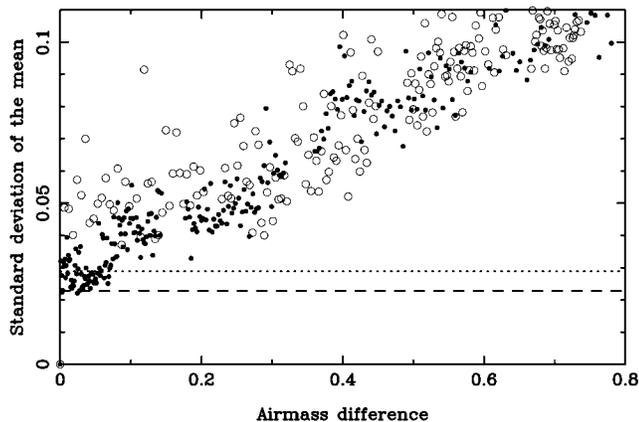
FIG. 4.—Standard deviation of the mean of the ratio of a standard star taken at two different air masses over a wavelength range of 2.0584–2.0636 μm relative to an air mass of 1.13 (*filled circles*) and relative to an air mass of 1.94 (*open circles*). The dashed line represents the theoretical S/N attainable for observations at an air mass of 1.13; the dotted line is the same, but for an air mass of 1.94.

4.2. Removing the Residual Telluric Line Features in Oversampled Spectra

Figure 6 shows the He I absorption in a O7 Ib supergiant using data taken on 2003 June 7 UT. The supergiant is HD 192639, observed at 1116 UT at an air mass of 1.21, and the reference star is HD 195050, observed at 1050 UT at an air mass of 1.36. The spectra are wavelength-calibrated using the telluric absorption lines. The broad stellar absorption is clearly visible after dividing out the telluric lines. The residual spikes are due to the change in air mass and the telluric profile structure between the two exposures.

We investigate different methods for removing the residuals; these include simple Fourier filtering, clipping, and modeling.

We oversample our spectra above the Nyquist frequency of 2.5 pixels per spectrally resolved element, and our measured sampling (the instrumental profile) is 4.0 pixels. This, then, is the narrowest feature that the spectrograph can resolve for any spectral line source. The telluric residuals in Figure 6 arise from small changes in the shape of the line profile of the telluric absorption, and subsequent division of the science object by the standard source gives rise to large flux changes over very small wavelength intervals. These are usually smaller than the instrumental profile and can be readily identified in the final spectra. By comparing the results to a known list of telluric absorption lines and to the standard star spectrum, regions of poor S/N corresponding to the core of the telluric lines can be identified and interpolated over using a low-pass filter.

Another hypothesis is that the large residual spikes are due to systematic wavelength shift errors between to the two spectra. To study the effect of introducing a systematic wavelength shift in one of the two spectra, we take a detailed portion of the spectrum in Figure 6 and add a wavelength offset to the
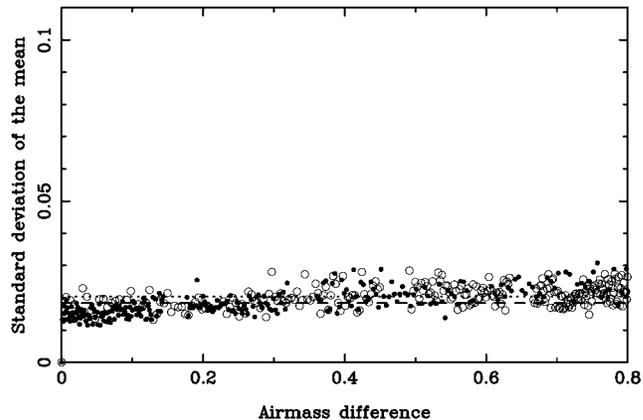
FIG. 5.—Same as Fig. 4, but over the range of 2.0602–2.0608 μm.

science star spectrum before dividing by the standard star. The results of adding a range of shifts are shown in Figure 7. Clear P Cygni–type profiles appear for even small wavelength offsets, indicating that accurate wavelength calibration is necessary for high spectral resolution work of this type. On the righthand side of the spectrum, telluric residuals of up to 40% of the continuum remain for all displayed shifts, while other telluric lines cancel out to give a flat continuum at other wavelengths. We confirmed this by dividing the A-star spectra at air masses similar to those of HD 192639 and its standard star, confirming the need to match air masses of scientific targets.

The almost constant wavelength spacing of the telluric lines in the rovibrational bands suggests that some form of Fourier filtering is needed to remove the residuals. We find that there is no effective way to remove all the residual lines without degrading the line profile on astrophysical lines of interest, so we do not recommend Fourier filtering as an effective way to remove the residuals. It is best to manually interpolate over
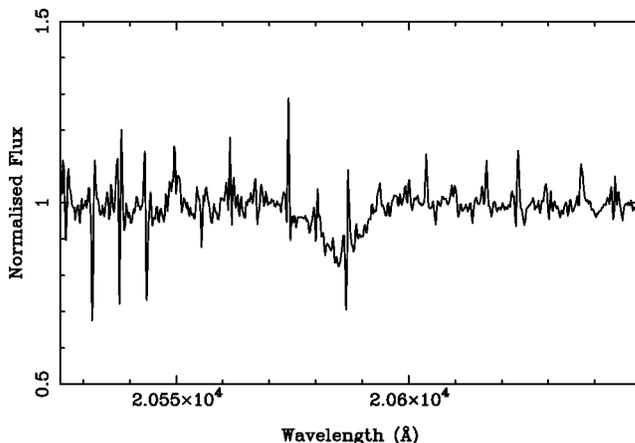
FIG. 6.—Spectrum of HD 192639. Residuals from the division of the standard are visible, along with the broad absorption from He I at 2.058 μm.
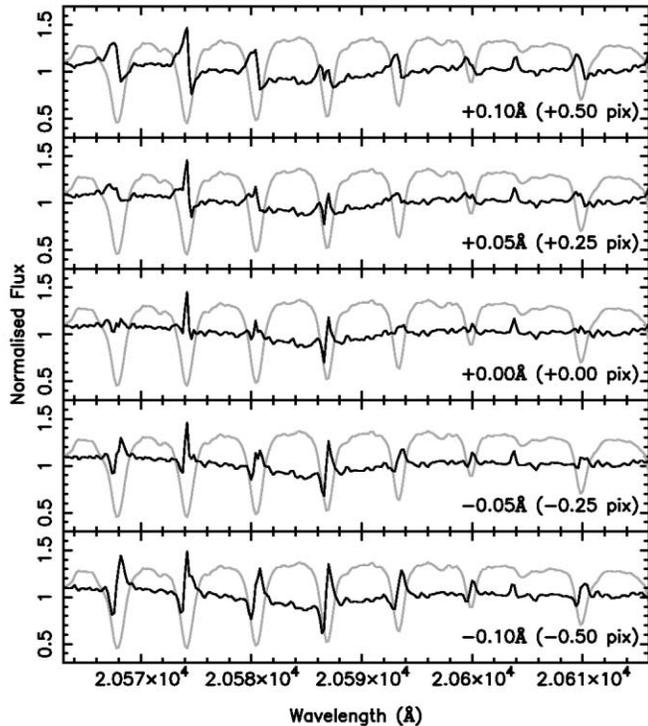
FIG. 7.—Spectrum of HD 192639 as a function of different wavelength misalignments. In each panel, the spectrum of HD 192639 is offset by the amount indicated in the lower right corner before division by the standard star spectrum. The standard star spectrum is shown in light gray to the same scale and with a flux offset of +0.3.

known telluric absorption features and then use a piecewise spline to supply replacement values over regions of low S/N.

5. CONCLUSIONS

The near-infrared spectral region provides a number of diagnostic transitions that are important in the analysis of a va-riety of astronomical objects. Yet ground-based observations are plagued by the need to remove of numerous, varying, and sometimes very strong absorption features originating in the Earth's atmosphere. Here we investigate telluric absorption as a function of air mass. Naturally, within the limit of bright stars and high spectral resolution, the greater the air-mass difference between the science target and the reference star, the lower the resulting S/N achieved in the final spectrum, and the greater the contamination of systematic residuals from the telluric-line wings. However, we also show that observations at higher air masses are degraded because of the larger rate of change of air mass with time and with the greater path length through the atmosphere. We find that a S/N of 20 (5%) is achievable for targets at air masses of around 1.9, increasing to a S/N of 50 (2%) for observations near an air mass of 1.15.

We conclude that high-S/N (100 and greater) spectra of as-trophysical spectral lines whose wavelengths and line widths coincide with the cores and widths of some of the deepest telluric absorption is impossible to achieve with the observing technique described in this paper. The variability of the telluric lines, combined with the large flux attenuation and necessarily long integration times, mean that only simultaneous observations with standards can compensate for the effects of the atmosphere.

By using high spectral resolution spectra, regions of low absorption between the telluric lines are able to reach near-photon-limited sensitivities (down to 1%), and for spectral features that are significantly broader than telluric features, high-S/N spectra are possible.

REFERENCES

Depoy, D. L., & Shields, J. C. 1994, ApJ, 422, 187

Greene, T. P., Tokunaga, A. T., Toomey, D. W., & Carr, J. S. 1993, Proc. SPIE, 1946, 313

Hanson, M. M., Conti, P. S., & Rieke, M. J. 1996, ApJS, 107, 281

Lord, S. D. 1992, A New Software Tool for Computing Earth's Atmospheric Transmission of Near- and Far-Infrared Radiation (NASA Tech. Memo. 103957; Moffett Field: Ames Research Center)

Lumsden, S. L., Puxley, P. J., & Hoare, M. G. 2001, MNRAS, 320, 83

Lumsden, S. L., Puxley, P. J., Hoare, M. G., Moore, T. J. T., & Ridge, N. A. 2003, MNRAS, 340, 799

Maiolino, R., Rieke, G. H., & Rieke, M. J. 1996, AJ, 111, 537

Porter, J. M., Drew, J. E., & Lumsden, S. L. 1998, A&A, 332, 999

Rothman, L. S., et al., 2003, J. Quant. Spectrosc. Radiat. Transfer, 82, 5

Rousselot, P., Lidman, C., Cuby, J.-G., Moreels, G., & Monnet, G. 2000, A&A, 354, 1134

Santolaya-Rey, A. E., Puls, J., & Herrero, A. 1997, A&A, 323, 488

Tokunaga, A. T. 1999, Allen's Astrophysical Quantities, ed. A. N. Cox (4th ed.; New York: AIP), 143

Vacca, W. D., Cushing, M. C., & Rayner, J. T. 2003, PASP, 115, 389